# A FDTD Surface Impedance Boundary Condition Using Z-Transforms

John H. Beggs
Mississippi State University
Department of Electrical and Computer Engineering
Box 9571
Mississippi State, MS 39762

## Abstract

*The surface-impedance boundary condition for the Finite-Difference, Time-Domain (FDTD) method is reformulated using digital filtering theory and Z transforms. The approach expands upon recent work in developing an efficient surface-impedance boundary condition for FDTD. The present work involves formulating the surface-impedance boundary condition in the frequency domain for a lossy dielectric half-space and for a thin lossy dielectric layer backed by a perfect conductor. The impedance function of the lossy medium is approximated with a series of low-pass filters. This approximation is independent of material properties and these low-pass filters are converted to corresponding digital filters using Z-transform theory. The FDTD surface-impedance boundary condition is reformulated in the Z domain, and the corresponding time-domain electric field sequence updating equation involves a recursive formula. Results are presented for both one and two-dimensional test problems.*

## 1 Introduction

The surface-impedance boundary condition (SIBC) is a frequency-domain concept that is used to simplify scattering calculations by eliminating the internal volume of lossy dielectric objects. The SIBC relates tangential electric and magnetic field components at the surface of the object through an impedance which is a function of the object's material parameters. Thus, the material properties of the object are accounted for, and if exterior fields are only of interest, the SIBC eliminates the need to calculate fields inside the scatterer. This results in a savings in computational resources by reducing the computational storage requirements and/or computation time.

To analyze electromagnetic field interaction with lossy dielectric objects, the Finite-Difference, Time-Domain (FDTD) method requires that the interior of the object be modeled in order for fields to penetrate the body. Since the wavelength inside a lossy dielectric material is much less than the free space wavelength, accurate modeling often requires a fine spatial grid resulting in a relatively large number of cells for moderately sized objects. For calculations where only exterior response is of interest, a conducting dielectric object can be replaced by a SIBC over the surface of the object. Thus, this boundary condition eliminates the spatial quantization of the object and reduces the overall size of the solution space by eliminating cells within the object and by allowing larger cells to be used in the exterior region. The larger cells reduce the storage requirements since fewer cells are required to model the same physical dimensions of the object. The computation time for the reduced solution space is also decreased because fields in cells within the object are not updated.

Most applications of the SIBC have traditionally been in the frequency domain [1]–[18]. Recently, time-domain surface-impedance concepts have received considerable attention in the literature [19]. There have been several FDTD implementations of the surface-impedance boundary condition introduced by various authors [20]–[38]. Each implementation has certain advantages and disadvantages, but all strive to obtain the most efficient and accurate method. These FDTD surface-impedance boundary conditions are reviewed in a separate article [39].

It has been demonstrated recently that dispersive and nonlinear optical media can be modeled in FDTD using digital filtering and Z-transform theory [40]. Materials with Debye or Lorentz dispersion have rational functions of frequency for the dielectric permittivity. These functions that define relative permittivities as a function of frequency have direct Z-transforms, thus allowing the relationship between electric flux density and field intensity to be formulated directly in the Z-domain. The resulting time-domain updating equations for the sequences involve recursive formulas and are computationally identical to the time-domain, differential-equation based meth-

ods. Excellent results have been obtained in modeling Debye, Lorentz and nonlinear optical media. The difficulty in applying Z-transform theory to the surface-impedance boundary condition is that the frequency-domain, surface-impedance function is irrational. With the recent work of Oh *et al.* [37], the normalized irrational surface-impedance function is approximated with a series of first-order, rational functions. This approximation is independent of material properties, and the first-order, rational functions can be transformed into an equivalent Z-domain form. This paper extends the work in [37] by providing the technical approach for reformulating the surface-impedance boundary condition using digital filtering and Z-transform theory. The surface-impedance boundary condition is converted to the Z-domain by two methods and the resulting recursive updating formulas for the electric field intensity sequence are almost computationally identical to that in [37]. There are several advantages of using the Z-transform approach to implement the SIBC for the FDTD method. The Z-transform approach provides a more accurate, intuitive and consistent method to implement the SIBC based upon the discrete nature of the FDTD method. In the traditional recursive convolution approach, the SIBC is implemented by convolving analog time-domain impedance and magnetic field signals that have been discretized in time. However, the discrete nature of the FDTD method results in discrete impedance and magnetic field *sequences* which are manipulated easily and accurately using Z-transforms. The Z-domain SIBC system functions are digital filters that operate on the discrete FDTD magnetic field sequences which provides a more accurate implementation and a more intuitive and cohesive theoretical formulation.

In this paper, Section 2 develops the surface impedance boundary condition in the Z-domain and provides the recursive updating equations for the electric field intensity sequence for both a lossy dielectric half-space and a thin lossy dielectric layer backed by a perfect electrical conductor (PEC). Section 3 presents one- and two-dimensional results, and Section 4 provides concluding remarks.

# 2 Z Transform Approach

This section develops the Z-transform approach for both a lossy dielectric half-space and a thin, PEC-backed, lossy-dielectric layer. The planar first-order, frequency-domain SIBC is used and then an efficient implementation of the corresponding time-domain SIBC is developed using digital filtering and Z-transform theory. This approach is an extension of previous work by Oh *et al.* [37] in developing an efficient time-domain SIBC using recursion. The notation presented in that paper [37] has been preserved as much as possible in the present work.

## 2.1 Lossy Dielectric Half-Space

The first-order (or Leontovich) impedance boundary condition relates tangential total field components and is given in the frequency domain as [4]

$$\vec{E}(\omega) - \hat{n}\left[\hat{n}\cdot\vec{E}(\omega)\right] = Z_s(\omega)\left[\hat{n}\times\vec{H}(\omega)\right] \quad (1)$$

where $\omega$ is the radian frequency, $\hat{n}$ is the unit outward normal from the surface and $Z_s(\omega)$ is the frequency-domain surface-impedance of the material. An $e^{j\omega t}$ time dependence is assumed and suppressed. This frequency-domain SIBC is for a planar material interface and does not account for the surface curvature of an object. Since the present formulation uses the planar SIBC, it is limited to those geometries where the smallest radius of curvature is relatively large compared to the wavelength. The frequency-domain surface-impedance is given by

$$Z_s(\omega) = \sqrt{\frac{j\omega\mu}{\sigma + j\omega\epsilon}} \quad (2)$$

When the impedance boundary is between free space and the dielectric, it is assumed that the complex refractive index, $N$, obeys the restriction

$$|N| \gg 1 \quad (3)$$

where $N = \sqrt{\mu_r\hat{\epsilon}_r(\omega)}$. This restriction is imposed so that the wave impedance in the material is independent of the incidence angle and will be equal for both polarizations. This restriction limits the applicability of the present formulation to those media with large conductivity or permittivity, but this restriction is feasible for most practical simulations where a SIBC would be applicable. For cases of low $|N|$, the approach developed by Kellali *et al.* [29] includes the incidence angle in the SIBC. That formulation may be beneficial in cases of lower $|N|$ to avoid gridding and updating fields within a large object. Since the restriction of (3) holds, then (2) is applicable for both polarizations in the two- and three-dimensional cases. This implies that the transmitted fields inside the object will propagate almost normal to the object surface; hence the wave impedance will be equal for both polarizations.

The frequency-domain surface-impedance function of (2) can be rewritten using the complex frequency variable $s = j\omega$ as

$$Z_s(s) = Z_i\sqrt{\frac{s}{s+a}} \quad (4)$$

where $a = \sigma/\epsilon$ and $Z_i$ is the intrinsic wave impedance of the material given by $Z_i = \sqrt{\mu/\epsilon}$. Following the procedure in [37], equation (4) can be rewritten as a normalized

impedance function given by

$$Z_n(s') = \frac{Z_s(s')}{Z_i} = \sqrt{\frac{s'}{s'+1}} \tag{5}$$

where $s' = s/a$. The normalized surface-impedance function is approximated in the frequency domain by a series of first order rational functions of the form

$$Z_n(s') \approx 1 - \sum_{l=1}^{L} \frac{C_l}{s' + \omega_l} \tag{6}$$

This approximation is over the real axis interval $s' = [0, 3]$, which will accommodate most materials up to several tens of Gigahertz. The residues $C_l$ and poles $\omega_l$ are given for sixth, seventh and eighth-order approximations in [37]. Figure 1 shows the percentage error for the eighth-order approximation, which will be used throughout this paper. Using the approximation in (6),

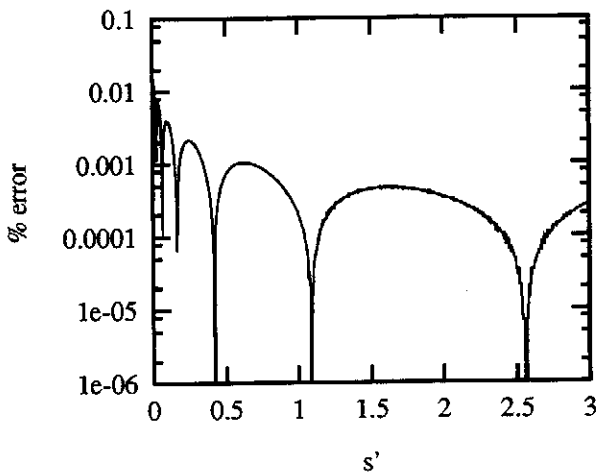


Figure 1: Percent error versus complex frequency ($s'$) in eighth-order approximation to surface impedance function.

the frequency-domain, surface-impedance function can be written as

$$Z_s(s) \approx Z_i - \sum_{l=1}^{8} \frac{aZ_iC_l}{s + a\omega_l} \tag{7}$$

The time-domain, surface-impedance boundary condition is obtained by applying the Convolution Theorem to (1) which results in

$$\vec{e}_t(t) = z_s(t) \otimes \left[\hat{n} \times \vec{h}(t)\right] \tag{8}$$

where the $\otimes$ is the convolution operator, $\vec{e}(t)$ and $\vec{h}(t)$ are the time-domain electric and magnetic field intensities at the impedance boundary and the subscript '$t$' denotes tangential field. From (7), it is clear that the time-domain representation of each first-order rational function is a decaying exponential. As a result, the convolution with the tangential magnetic field can be updated using recursion to avoid storing the complete time history of the magnetic field at the material interface. This recursive approach was first proposed in [22]-[23] and has been expanded upon by several authors [29]–[31], [34]–[38]. Sullivan [41] has shown the multiplication theorem for convolution involving FDTD discrete field sequences includes the sampling factor $T$. Thus the Z-domain surface-impedance boundary condition is given by

$$\vec{E}_t(z) = Z_s(z)\left[\hat{n} \times \vec{H}(z)\right] T \tag{9}$$

Each of the first-order rational functions in (7) is a low-pass filter. When an analog filter function is known, digital filters can be obtained directly using three different approaches [42]. These approaches are discussed in the following sections.

### 2.1.1 Impulse Invariance Method

The first approach to obtaining a digital filter from an analog filter is to use the impulse-invariance procedure which involves choosing the unit sample response of the digital filter as equally spaced samples of the impulse response of the analog filter. The time-domain, surface-impedance impulse response is found via an inverse Laplace transform of the frequency-domain expression in (7) to be

$$z_s(t) = Z_i\delta(t) - \sum_{l=1}^{8} aC_l e^{-a\omega_l t} \tag{10}$$

where $\delta(t)$ is the Dirac delta function. If this time-domain impulse response is now sampled with interval $T$, the discrete surface-impedance impulse response is

$$z_s(n) = z_s(nT) = Z_i\delta(nT) - \sum_{l=1}^{8} aC_l e^{-a\omega_l nT} \tag{11}$$

Taking the Z-transform of both sides of this equation gives the Z-domain, surface-impedance function of

$$Z_s(z) = \frac{Z_i}{T} - \sum_{l=1}^{8} \frac{aC_l}{1 - z^{-1}e^{-a\omega_l T}} \tag{12}$$

The Z-domain surface-impedance boundary condition of (9) is then

$$\vec{E}_t(z) = \left[Z_i - \sum_{l=1}^{8} \frac{aC_lT}{1 - z^{-1}e^{-a\omega_l T}}\right]\left[\hat{n} \times \vec{H}(z)\right] \tag{13}$$

This equation can be rewritten after some algebra as

$$\vec{E}_t(z) = Z_i \left[\hat{n} \times \vec{H}(z)\right] - \sum_{l=1}^{8} \vec{F}_l(z) \qquad (14)$$

where

$$\vec{F}_l(z) = e^{-a\omega_l T} z^{-1} \vec{F}_l(z) + aC_l Z_i \left[\hat{n} \times \vec{H}(z)\right] \qquad (15)$$

is the recursive updating equation in the Z-domain. Recall that the $z^{-1}$ term is a delay operator, and in the time domain, these equations become

$$\vec{e}_t^{\,n}(k) = Z_i \left[\hat{n} \times \vec{h}^{n-1/2}(k-1/2)\right] - \sum_{l=1}^{8} \vec{f}_l^{\,n}(k) \qquad (16)$$

with

$$\begin{aligned} \vec{f}_l^{\,n}(k) &= e^{-a\omega_l T} \vec{f}_l^{\,n-1}(k) \\ &\quad + aC_l Z_i \left[\hat{n} \times \vec{h}^{n-1/2}(k-1/2)\right] \end{aligned} \qquad (17)$$

as the recursive updating equation suitable for FDTD implementation. Note that equation (16) is identical to equation (8a) in [37] with a minor change in notation. By using the impulse invariance procedure, it is assumed that the field sequences are piecewise constant in time. This will result in only a first-order accurate boundary condition, similar to the recursive convolution approach for dispersive media involving piecewise constant field components. When implemented and tested, the impulse invariance procedure led to instabilities because of the aliasing problems in the digital filter frequency response, and because the time step chosen for the FDTD calculations was not small enough to resolve the characteristic time constants of some of the exponential terms in the unit impulse response. It is interesting to note that the impulse-invariance design approach was shown to be unstable for FDTD modeling of dispersive media for certain materials exhibiting Lorentz dispersion [43]. Therefore, no results are shown using the impulse-invariance procedure, but this section was included for completeness and for comparison to the other Z-domain methods.

### 2.1.2 Backward Difference Method

With the frequency-domain surface-impedance of (7), the surface-impedance boundary condition can be rewritten to be

$$\vec{E}_t(s) \approx \left[Z_i - \sum_{l=1}^{8} \frac{aC_l Z_l}{s + a\,\omega_l}\right] \left[\hat{n} \times \vec{H}(s)\right] \qquad (18)$$

The backward difference method is a digital filter design technique based upon the numerical solution of a differential equation. Each of the first-order rational terms above can be thought of as the analog system function for a first-order time-domain differential equation. By approximating the time derivatives in the differential equation by a backward difference, the digital system function is obtained from the analog system function by a substitution of variables

$$s = \frac{1 - z^{-1}}{T} \qquad (19)$$

Substituting this into (18) and after some manipulation gives the Z-domain surface-impedance boundary condition

$$\begin{aligned} \vec{E}_t(z) \;\approx\; & \left[Z_i - \sum_{l=1}^{8} \frac{a\,C_l\,Z_i\,T}{(1 - z^{-1}) + a\,\omega_l\,T}\right] \cdot \\ & \left[\hat{n} \times \vec{H}(z)\right] \end{aligned} \qquad (20)$$

Note that an extra $T$ term does not appear above because this transformation does not involve the convolution theorem, hence the $T$ factor is not present. After some algebra, equation (20) can be written in the form

$$\vec{E}_t(z) = Z_i \left[\hat{n} \times \vec{H}(z)\right] - \sum_{l=1}^{8} \vec{F}_l(z) \qquad (21)$$

where

$$\vec{F}_l(z) = \frac{z^{-1}}{1 + a\omega_l T} \vec{F}_l(z) + \frac{aC_l Z_i T}{1 + a\omega_l T} \left[\hat{n} \times \vec{H}(z)\right] \qquad (22)$$

is the recursive updating equation in the Z-domain. The time-domain SIBC is the same as that given in (16) with

$$\begin{aligned} \vec{f}_l^{\,n}(k) &= \frac{1}{1 + a\omega_l T} \vec{f}_l^{\,n-1}(k) \\ &\quad + \frac{aC_l Z_i T}{1 + a\omega_l T} \left[\hat{n} \times \vec{h}^{n-1/2}(k-1/2)\right] \end{aligned} \qquad (23)$$

as the recursive updating equation suitable for FDTD implementation.

### 2.1.3 Bilinear Transformation Method

If the time-domain differential equation used for the backward difference method for each of the first-order rational functions in (18) is integrated, and then this integral is approximated by the trapezoidal rule, the corresponding Z-domain system function can be obtained from the analog function by a different substitution of variables. This is the bilinear transformation method, and the substitution of variables is

$$s = \frac{2}{T} \frac{1 - z^{-1}}{1 + z^{-1}} \qquad (24)$$

Performing this substitution of variables in (18) and after some algebra gives the Z-domain surface-impedance

boundary condition to be

$$\vec{E}_t(z) \approx [Z_i - \sum_{l=1}^{8} \frac{a\,C_l\,Z_i\,T\,(1+z^{-1})}{(2+a\omega_l T)-(2-a\omega_l T)\,z^{-1}}] \left[\hat{n}\times\vec{H}(z)\right] \quad (25)$$

Note that an extra $T$ term does not appear above because the bilinear transformation does not involve the convolution theorem, hence the $T$ factor is not required. Equation (25) can be written in the same form as (14) where

$$\vec{F}_l(z) = \left(\frac{2-a\,\omega_l T}{2+a\,\omega_l T}\right) z^{-1}\,\vec{F}_l(z) + \left(\frac{aC_l Z_i T}{2+a\,\omega_l T}\right)(1+z^{-1})\left[\hat{n}\times\vec{H}(z)\right] \quad (26)$$

is the recursive updating equation in the Z-domain. The corresponding time-domain SIBC update equation is the same as (16) and the recursive time-domain update equation is given by

$$\vec{f}_l^{\,n}(k) = \left(\frac{2-a\,\omega_l T}{2+a\,\omega_l T}\right)\vec{f}_l^{\,n-1}(k) + \left(\frac{aC_l Z_i T}{2+a\,\omega_l T}\right)\left[\hat{n}\times\left(\vec{h}^{\,n-1/2}(k-1/2) + \vec{h}^{\,n-3/2}(k-1/2)\right)\right] \quad (27)$$

and is suitable for FDTD implementation. In the paper by Oh *et al.*, the recursive updating equation is given by equation (8b) of that paper [37] (with a slight change of notation) as

$$\vec{e}_i^{\,n}(k) = Z_i\left[\hat{n}\times\vec{h}^{\,n-1/2}(k-1/2)\right] - \sum_{l=1}^{8}\vec{A}_i^{\,n}(k) \quad (28)$$

where $\vec{A}_i^{\,n}(k)$ is the recursive updating variable given by

$$\vec{A}_i^{\,n}(k) = \frac{Z_i C_i}{\omega_i}\left[1+\left(e^{-a\omega_i T}-1\right)/(a\omega_i T)\right]\cdot \left[\hat{n}\times\vec{h}^{\,n-1/2}(k-1/2)\right] + \frac{Z_i C_i}{\omega_i}\left[1/(a\omega_i T) - e^{-a\omega_i T}(1+1/(a\omega_i T))\right]\cdot \left[\hat{n}\times\vec{h}^{\,n-3/2}(k-1/2)\right] + e^{-a\omega_i T}\vec{A}_i^{\,n-1}(k) \quad (29)$$

The coefficients of this recursive updating equation were obtained by *directly* evaluating the convolution integral of the time-domain surface-impedance function with the tangential magnetic field next to the impedance boundary. The coefficients in (17), (23) and (27) were obtained by manipulating the surface-impedance function in the Z-domain. All of the coefficients in the recursive updating equations of (17), (23), (27) and (29) can be precomputed and stored to maximize efficiency. Comparing the coefficients in (17), (23) with (29), it is clear that the former two equations are first-order accurate since they only involve one past time level of the tangential magnetic field. Note that the bilinear transformation recursion equation in (27) requires one less multiply and one less coefficient storage location per recursive updating variable than the equation in (29). This makes the bilinear transformation approach slightly more efficient than (29). The bilinear transformation maps the entire left half of the complex plane inside the unit circle and the imaginary axis in the complex plane becomes the unit circle. As a result, frequency warping will take place when transferring from the analog system to the digital system. The bilinear transformation is most useful when this distortion can be tolerated or compensated. When designing a digital filter using the bilinear transformation, the analog cutoff frequencies can be prewarped so that the digital cutoff frequencies will fall at the correct design cutoff frequencies. However, in this application, this distortion in the frequency axis can be tolerated and no compensation is required.

## 2.2 PEC-Backed Thin Lossy Dielectric Layer

Following the notation in [37], this section develops a Z-transform SIBC implementation for a PEC-backed, thin, lossy dielectric layer. The geometry is one-dimensional and the lossy dielectric layer has thickness, $d$, and parameters $\epsilon_l$, $\mu_l$ and $\sigma_l \neq 0$. It is assumed that the intrinsic impedance of the dielectric layer, $Z_i(\omega)$, (equation (2)) obeys the restriction given in (3) and that $d$ is less than one-half the cell size. Since the dielectric layer is backed by a PEC, the surface impedance looking into the layer is

$$Z_s(\omega) = Z_i(\omega)\tan(\gamma(\omega)d) \quad (30)$$

where $\gamma(\omega)$ is the propagation constant. If $d$ is small, then the approximation

$$\tan(\gamma(\omega)d) \approx \gamma(\omega)d \quad (31)$$

is applied to (30) to give

$$Z_s(\omega) = Z_i(\omega)\gamma(\omega)d = j\omega\mu_l d \quad (32)$$

Using the Laplace transform variable $s = j\omega$ gives

$$Z_s(s) = \mu_l d s \quad (33)$$

Now that the thin-layer surface-impedance is expressed in terms of $s$, the Z-transform methods can be applied directly to obtain the corresponding update equations.

### 2.2.1 Backward Difference Method

For the backward difference method, the substitution of variables given in (19) is used in (33) to give

$$Z_s(z) = \mu_l d \left( \frac{1 - z^{-1}}{T} \right) \tag{34}$$

in the Z-domain. Now the Z-domain SIBC can be written as

$$\vec{E}_t(z) = \frac{\mu_l d}{T} \left[ \left(1 - z^{-1}\right) \left( \hat{n} \times \vec{H}(z) \right) \right] \tag{35}$$

and the time-domain SIBC is given by

$$\begin{aligned} \vec{e}_t^{\,n}(k) &= \frac{\mu_l d}{T} \left[ \hat{n} \times \left( \vec{h}^{n-1/2}(k - 1/2) \right. \right. \\ &\quad \left. \left. - \vec{h}^{n-3/2}(k - 1/2) \right) \right] \end{aligned} \tag{36}$$

which is suitable for FDTD implementation. Note that this update equation is identical to (12) in [37]. The backward difference method is the only stable Z-transform method for the PEC-backed, lossy dielectric layer. The bilinear transformation method was unstable because the resulting Z-domain surface-impedance function has a pole at $\Omega = \pi$ where $\Omega$ is the digital filter frequency variable.

# 3 Demonstration

## 3.1 Lossy Dielectric Half-Space

To demonstrate these different approaches, equation (16), along with the recursive updating equations, (23) and (27) were implemented in a one-dimensional total field FDTD code for the geometry shown in Figure 2. The

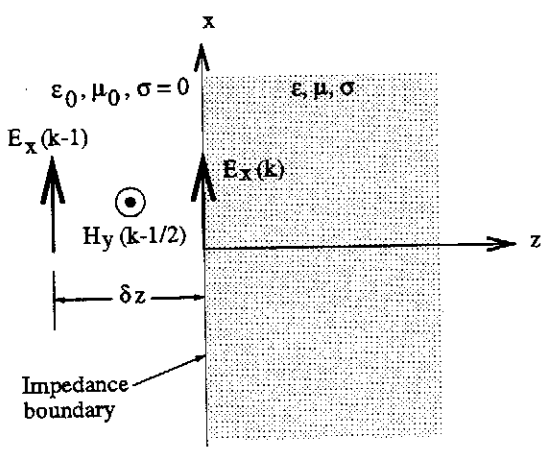


Figure 2: Problem geometry for FDTD SIBC with one-dimensional FDTD grid and the placement of the impedance boundary.

problem was to calculate the reflection coefficient versus frequency for a pulse normally incident on a lossy dielectric half space. The problem space size was 100 cells, the impedance boundary was located at cell 100 and the electric field was sampled at cell 100. The maximum frequency of interest was 10 GHz and the incident electric field was a Gaussian pulse with unity amplitude of the form

$$E_x^i(t) = e^{-((t-t_0)/\tau)^2} u(t) \tag{37}$$

with $t_0 = 80$ ps and $\tau = 20$ ps. The pulse was windowed in time at approximately -80 dB with a rectangular window width of 64 time steps. The frequency response of the pulse contained significant energy to 12 GHz. Two computations were made with $\sigma = 2.0$ S/m and $\sigma = 200.0$ S/m corresponding to loss tangents at 10 GHz of 3.6 and 360, respectively. The permittivity and permeability of the lossy dielectric half space were taken as those of free space. The cell size and time step were 750 $\mu$m (40 cells/$\lambda_0$ at 10 GHz) and 2.5 ps respectively, and a total of 8192 time steps were evaluated. For each FDTD computation, a reflection coefficient versus frequency was obtained by dividing the Fourier transform of the scattered field by the Fourier transform of the incident field at cell 100. The incident field was obtained by running the FDTD code with free space only and recording the electric field at cell 100. The scattered field is then obtained by subtracting the time-domain incident field from the time-domain total field. The results are compared with the analytic surface-impedance reflection coefficient computed from

$$|R| = \left| \frac{1 - \sqrt{1 - j\sigma/\omega\epsilon_0}}{1 + \sqrt{1 - j\sigma/\omega\epsilon_0}} \right| \tag{38}$$

where $\sigma$ is the conductivity of the dielectric half-space. The Z-transform results are also compared with the direct recursive convolution approach of Oh *et al.* [37] using the eighth order approximation and with a conventional FDTD calculation for a simulated lossy half-space. In all figures, the following abbreviations apply: recursive convolution, RC; backward difference, BD; bilinear transformation, BLT. Figures 3 and 4 show the SIBC reflection coefficient results for all methods compared with the analytic SIBC result for $\sigma = 2.0$ S/m and $\sigma = 200.0$ S/m, respectively. Notice the agreement is excellent for the $\sigma = 2.0$ case and is less at higher frequencies in the $\sigma = 200.0$ case. This discrepancy is due to discretization error. In Figure 4, note that the SIBC implementations have approximately the same absolute accuracy as the FDTD result and the SIBC cannot be expected to perform any better than the FDTD calculation. Therefore, these results are encouraging. Comparing Figure 4 to Figure 3c in [37], it is clear that Figure 3c exhibits better agreement at higher frequencies. However, this is because the reflection coefficient shown in that graph was computed

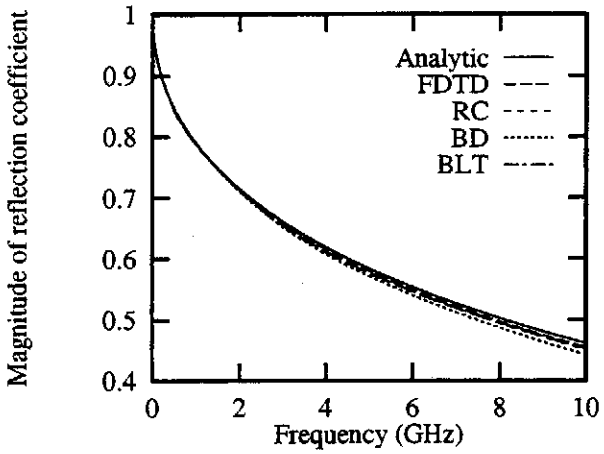


Figure 3: Reflection coefficient magnitude versus frequency for normal incidence plane wave reflection from a lossy dielectric half space with $\sigma$ = 2.0 S/m using the analytic and FDTD SIBC methods.

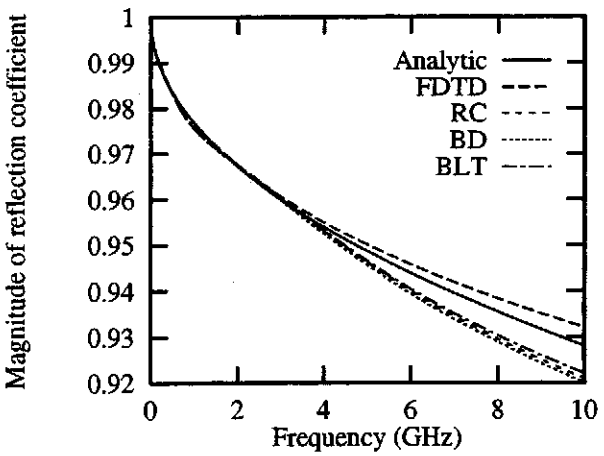


Figure 4: Reflection coefficient magnitude versus frequency for normal incidence plane wave reflection from a lossy dielectric half space with $\sigma$ = 200.0 S/m using the analytic and FDTD SIBC methods.

from a closed form representation for the rational function approximation. Note in Figure 4 from [37] that the results for the case of $\sigma$ = 2.0 S/m with a six-term rational function approximation exhibit the same type of high frequency behavior as the results presented in Figure 3 and Figure 4. Thus, the results presented here are consistent with those presented in [37]. The Z-transform SIBCs are only first-order accurate overall because the magnetic field at the impedance boundary is approximated by the magnetic field one-half cell in front of the impedance boundary. Although it was anticipated that the bilinear transformation method was second-order accurate in time, when applied in practice, it is only first-order accurate. This is illustrated in Figure 5 where the BLT method is used at a cell spacing of 325 $\mu$m (1/2 the previous cell size) with a conductivity of $\sigma$ = 200.0 S/m. Note that

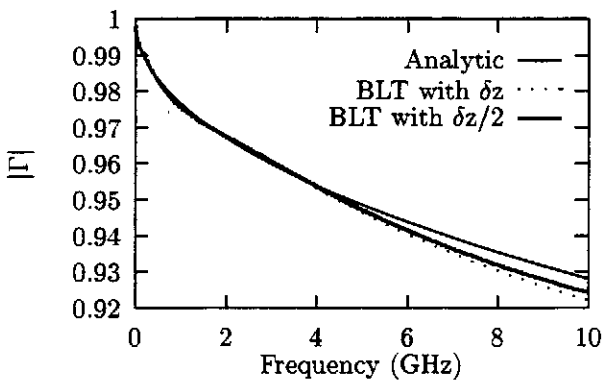


Figure 5: Reflection coefficient magnitude versus frequency for normal incidence plane wave reflection from a lossy dielectric half space with $\sigma$ = 200.0 S/m using the FDTD BLT SIBC at grid resolutions of $\delta z$ and $\delta z/2$.

the new result is approximately 50% closer to the analytical solution. Similar behavior was observed with the BD method.

## 3.2 PEC-Backed Thin Lossy Dielectric Layer

The calculation parameters for the thin layer example are the same as for the previous example except the material parameters have the following values:

$$\begin{aligned} \epsilon_l &= 2\epsilon_0 \\ \mu_l &= 2\mu_0 \\ \sigma_l &= 2.0\,\mathrm{S/m} \end{aligned} \tag{39}$$

and $d = 0.1\delta z$. In this example, the impedance is calculated at the thin-layer interface by calculating the ratio of the electric and magnetic fields computed via the SIBC.

This is then compared with the exact impedance value computed from (30). Excellent agreement is obtained for the BD Z-transform method as shown in Figure 6.

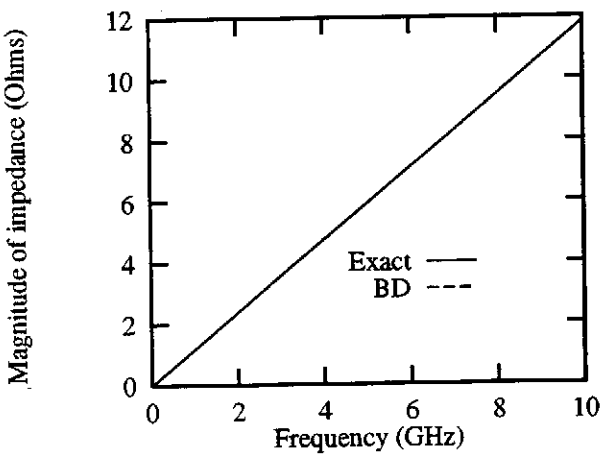


Figure 6: Magnitude of complex impedance for a thin, PEC-backed lossy dielectric layer with $\epsilon = 2\epsilon_0$, $\mu = 2\mu_0$, $\sigma = 2.0$ S/m and $d = 0.1\delta z$.

### 3.3 Two-Dimensional Scattering Example

In this example, a two-dimensional TM FDTD code was adapted to use the recursive convolution and Z-transform SIBCs. Figure 7 shows the two-dimensional geometry for both the plane wave and point source excitations. A plane wave is incident from the $-x$ axis

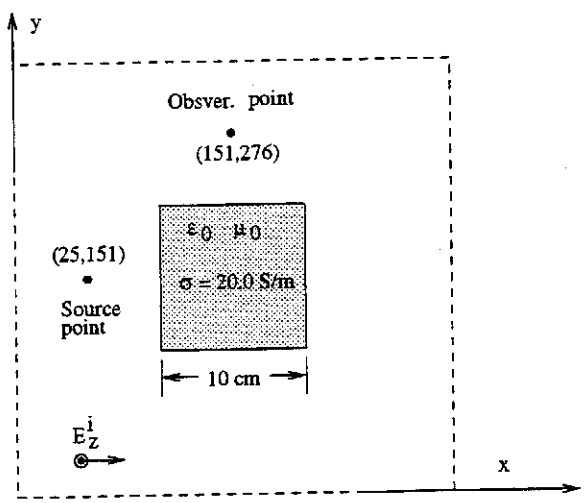


Figure 7: Problem geometry for two-dimensional TM scattering calculations showing square cylinder, incident plane wave, point source and field sampling points.

and a two-dimensional scattering width is calculated for a square cylinder. The cylinder is 10 cm square and has the following parameters: $\epsilon_r = 1$, $\mu_r = 1$ and $\sigma = 20.0$ S/m. The problem space size was 300 by 300 cells, the cell size is 500 $\mu$m and the time step is 1.2 ps. Scattering angles of $\phi = 180$, 90 and 0 degrees were used, where $\phi$ is measured from the $+x$ axis. The incident pulse was of the same form as (37) with $t_0 = 37.7$ ps and $\tau = 9.45$ ps and a second-order Liao absorbing boundary condition was used [44]. Since an analytical solution is not available, each Z-transform approach is compared with a conventional FDTD calculation for the same geometry. Figure 8 shows the monostatic scattering width at $\phi = 180°$ and Figures 9 and 10 show the bistatic scattering width at $\phi = 90°$ and $\phi = 0°$, respectively. Note the agreement is good in all three cases. It is interesting to note

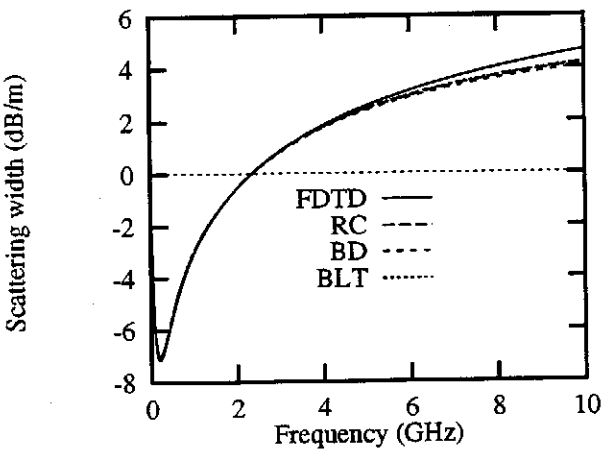


Figure 8: Monostatic scattering width at $\phi = 180°$ for lossy square cylinder using conventional FDTD and the various SIBC implementations.

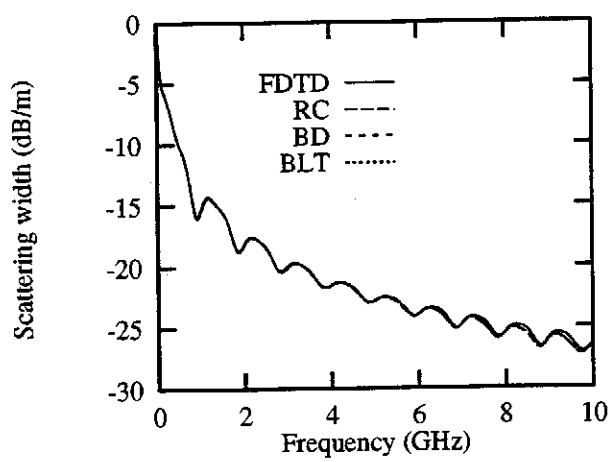


Figure 9: Bistatic scattering width at $\phi = 90°$ for lossy square cylinder using conventional FDTD and the various SIBC implementations.

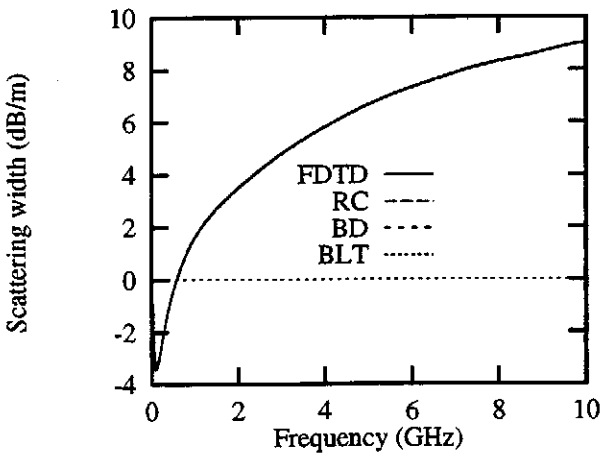


Figure 10: Bistatic scattering width at $\phi = 0°$ for lossy square cylinder using conventional FDTD and the various SIBC implementations.

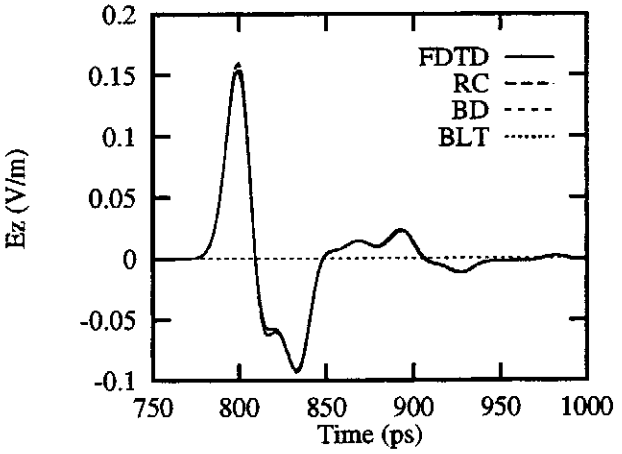


Figure 11: Near zone scattered electric field at a point 25 cells above a 10 cm lossy square cylinder with a point source excitation.

that the half-cell spacing error between electric and magnetic fields in the SIBC seems to manifest itself more in the monostatic scattering width of Figure 7 than in the bistatic scattering width patterns. This is most likely due to cancellation of the SIBC error sources from all four sides of the square cylinder in the bistatic directions. A nonplanar wave example was also used with the excitation point located at grid point $i_0, j_0$ (see Fig. 7) and a soft excitation source of the form

$$E_z^{total}(i_0, j_0) = E_z^{fdtd}(i_0, j_0) + E_z^{inc}(i_0, j_0) \qquad (40)$$

where $E_z^{fdtd}(i_0, j_0)$ is the free-space electric field updated using FDTD and $E_z^{inc}(i_0, j_0)$ is the source term of the same form as (37). The source point was located at $i_0 = 25, j_0 = 151$ and the pulse parameters were $t_0 = 37.7$ ps and $\tau = 9.45$ ps with the amplitude of the source at 1000 V/m. The results are shown in Figure 11 for a near-field sampling point located at grid point (151,276). Note the agreement is excellent for the recursive convolution method and for both Z-transform methods.

# 4 Conclusion

An efficient implementation of the frequency-dependent SIBC for the FDTD method based upon Z-transforms has been presented. Both the backward difference and bilinear transformation Z-transform methods were implemented and tested for a lossy dielectric half-space and the backward difference method was implemented and tested for a thin PEC-backed lossy dielectric layer. Excellent agreement was obtained on one- and two-dimensional TM problems using both plane and nonplanar wave excitations. Although only a square geometry was considered in the two-dimensional example in this paper, scattering from circular cylinders was demonstrated using a similar SIBC in [27]. The extension to the two-dimensional TE case and the three-dimensional case is straightforward.

## Acknowledgements

The author would like to thank the anonymous reviewers for their comments and suggested improvements for this paper.

# References

[1] M. A. Leontovich, "On the approximate boundary conditions for electromagnetic fields on the surface of well conducting bodies", in *Investigations of propagation of radio waves*, B. Vvedensky, Ed., pp. 5–20. Moscow: Academy of Sciences USSR, 1948.

[2] M. A. Leontovich, "Approximate boundary conditions for the electromagnetic field on the surface of a good conductor", in *Investigations on Radiowave Propagation*, V. A. Fock, Ed., pt. 2, pp. 5–12. Printing House of the Academy of Sciences, Moscow, 1957, Translation: V. A. Fock, *Diffraction refraction and reflection of radio waves*, Appendix, Air Force Cambridge Res. Center TN-57-102.

[3] Z. Godzinski, "The surface impedance concept and the structure of radio waves over real earth", *Proc. IEE*, vol. 108C, pp. 362–373, March 1961.

[4] T. B. A. Senior, "Impedance boundary conditions for imperfectly conducting surfaces", *Appl. Sci. Res. B*, vol. 8, pp. 418–436, 1960.

[5] T. B. A. Senior, "Impedance boundary conditions for statistically rough surfaces", *Appl. Sci. Res B*, vol. 8, pp. 437, 1960.

[6] S. N. Karp and Jr. F. C. Karal, "Generalized impedance boundary conditions with applications to surface wave structures", in *Electromagnetic Wave Theory*, J. Brown, Ed., pt. 1, pp. 479–483. Pergamon, New York, 1965.

[7] J. R. Wait and C. M. Jackson, "Calculations of bistatic scattering cross section of a sphere with an impedance boundary condition", *J. Res. NBS, USNC-RSI*, vol. 69D, no. 2, pp. 298–315, Feb. 1965.

[8] K. M. Mitzner, "An integral equation approach to scattering from a body of finite conductivity", *Radio Sci.*, vol. 2, no. 12, pp. 1459–1470, Dec. 1967.

[9] M. Ohkubo, "The surface impedance of a moving medium", *Elect. Comm. in Japan*, vol. 52-B, pp. 125–128, 1969.

[10] A. L. Weinstein, *The Theory of Diffraction and the Factorization Method*, Golem, Boulder, CO, 1969.

[11] N. G. Alexopoulos and G. A. Tadler, "Accuracy of the Leontovich boundary condition for continous and discontinuous surface impedances", *J. Appl. Phys.*, vol. 46, no. 8, pp. 3326–3332, August 1975.

[12] J. R. Wait, "Exact surface impedance for a cylindrical conductor", *Elec. Lett.*, vol. 15, no. 20, pp. 659–660, Sept. 1979.

[13] J. R. Wait, "Exact surface impedance for a spherical conductor", *Proc. IEEE*, vol. 68, pp. 279–281, Feb. 1980.

[14] T. B. A. Senior and J. L. Volakis, "Sheet simulation of a thin dielectric layer", *Radio Sci.*, vol. 22, pp. 1261–1272, 1987.

[15] D. Wang, "Limits and validity of the impedance boundary condition on penetrable surfaces", *IEEE Trans. Antennas Propagat.*, vol. AP-35, pp. 453–457, April 1987.

[16] T. B. A. Senior and J. L. Volakis, "Derivation and application of a class of generalized boundary conditions", *IEEE Trans. Antennas Propagat.*, vol. 37, no. 12, pp. 1566–1572, Dec. 1989.

[17] J. L. Volakis and T. B. A. Senior, "Applications of a class of generalized boundary conditions to scattering by a metal-backed dielectric half-plane", *Proc. IEEE*, vol. 77, pp. 796–805, May 1989.

[18] K. W. White and R. Mittra, "A systematic study of the impedance boundary condition", in *Proc. 1990 IEEE Antennas Propagat. Int. Symp.*, Dallas, TX, May 6–11 1990, pp. 870–873.

[19] F. M. Tesche, "On the inclusion of loss in time-domain solutions of electromagnetic interaction problems", *IEEE Trans. Electromagn. Compat.*, vol. EMC-32, pp. 1–4, Feb. 1990.

[20] J. G. Maloney and G. S. Smith, "Implementation of surface impedance concepts in the finite-difference TIme-domain (FD-TD) technique", in *IEEE Antennas and Propagat. Soc. Int. Symposium*, Dallas, TX, May 1990, vol. 4, pp. 1628–1631.

[21] D. J. Riley and C. D. Turner, "The inclusion of wall loss in finite-difference time-domain thin-slot algorithms", *IEEE Trans. Electromagn. Compat.*, vol. 33, no. 4, pp. 304–311, 1991.

[22] J. G. Maloney and G. S. Smith, "The use of surface impedance concepts in the finite-difference time-domain method", *IEEE Trans. Antennas Propagat.*, vol. 40, no. 1, pp. 38–48, 1992.

[23] J. H. Beggs, R. J. Luebbers, K. S. Yee, and K. S. Kunz, "Finite-difference time-domain implementation of surface impedance boundary conditions", *IEEE Trans. Antennas Propagat.*, vol. 40, no. 1, pp. 49–56, 1992.

[24] C. F. Lee, R. T. Shin, and J. A. Kong, "Time domain modeling of impedance boundary condition", *IEEE Trans. Microwave Theory Tech.*, vol. 40, no. 9, pp. 1847–1850, 1992.

[25] T. Kashiwa, O. Chiba, and I. Fukai, "A formulation for surface impedance boundary conditions using the finite-difference time-domain method", *Microwave Opt. Technol. Lett.*, vol. 5, no. 10, pp. 486–490, 1992.

[26] K. S. Yee, K. Shlager, and A. H. Chang, "An algorithm to implement a surface impedance boundary condition for FDTD", *IEEE Trans. Antennas Propagat.*, vol. 40, no. 7, pp. 833–837, 1992.

[27] J. H. Beggs, *Finite-Difference Time-Domain Implementation of Surface Impedance Boundary Conditions in One, Two, and Three Dimensions*, PhD thesis, The Pennsylvania State University, University Park, PA, 1993.

[28] J. H. Beggs and R. J. Luebbers, "Corrections to "Finite-difference time-domain implementation of surface impedance boundary conditions"", *IEEE Trans. Antennas Propagat.*, vol. 41, no. 1, pp. 118, 1993.

[29] S. Kellali, B. Jecko, and A. Reineix, "Implementation of a surface impedance formalism at oblique incidence in FDTD method", *IEEE Trans. Electromagn. Compat.*, vol. 35, no. 3, pp. 347–356, 1993.

[30] S. Kellali, B. Jecko, and A. Reineix, "Surface impedance boundary conditions at oblique incidence in FDTD", *Annales des Télécommunications*, vol. 48, no. 5/6, pp. 268–276, 1993.

[31] S. Kellali, B. Jecko, and A. Reineix, "Absorbing surface impedances of lossy layers in the finite difference time-domain method", *Annales des Télécommunications*, vol. 49, no. 3/4, pp. 154–158, 1994.

[32] B. Z. Wang, "Time-domain modeling of the impedance boundary condition for an oblique incident parallel-polarization plane wave", *Microwave Opt. Technol. Lett.*, vol. 7, no. 1, pp. 19–22, 1994.

[33] B. Z. Wang, "Time-domain modeling of the impedance boundary condition for an oblique incident perpendicular-polarization plane wave", *Microwave Opt. Technol. Lett.*, vol. 7, no. 8, pp. 355–359, 1994.

[34] S. Kellali, A. Reineix, P. Leveque, and B. Jecko, "Time-domain surface impedances of lossless debye media", *Annales des Télécommunications*, vol. 50, no. 7/8, pp. 705–710, 1995.

[35] C. W. Penney, R. J. Luebbers, and J. W. Schuster, "Scattering from coated targets using a frequency-dependent, surface impedance boundary condition in FDTD", in *11th Annual Review of Progress in Applied Computational Electromagnetics*, Monterey, CA, Mar. 1995, vol. 1, pp. 445–452.

[36] C. W. Penney, R. J. Luebbers, and J. W. Schuster, "A frequency dependent FDTD surface impedance for scattering", in *IEEE Antennas and Propagat. Soc. Int. Symposium*, Newport Beach, CA, June 1995, vol. 1, pp. 628–631.

[37] K. S. Oh and J. E. Schutt-Aine, "An efficient implementation of surface impedance boundary conditions for the finite-difference time-domain method", *IEEE Trans. Antennas Propagat.*, vol. 43, no. 7, pp. 660–666, 1995.

[38] C. Penney, R. J. Luebbers, and J. W. Schuster, "Scattering from coated targets using a frequency-dependent, surface impedance boundary condition in FDTD", *IEEE Trans. Antennas Propagat.*, vol. 44, no. 4, pp. 434–443, 1996.

[39] J.H. Beggs, "A brief summary of surface impedance boundary conditions for FDTD", in preparation.

[40] D. M. Sullivan, "Frequency-dependent FDTD methods using Z transforms", *IEEE Trans. Antennas Propagat.*, vol. 40, no. 10, pp. 1223–1230, 1992.

[41] D. M. Sullivan, "$Z$-transform theory and the FDTD method", *IEEE Trans. Antennas Propagat.*, vol. 44, no. 1, pp. 28–34, 1996.

[42] A. V. Oppenheim and R. W. Schafer, *Digital Signal Processing*, Prentice-Hall, 1975.

[43] C. Hulse and A. Knoesen, "Dispersive models for the finite-difference time-domain method: Design, analysis, and implementation", *J. Opt. Soc. Am., A Optics Image Sci. Vision*, vol. 11, no. 6, pp. 1802–1811, 1994.

[44] Z. P. Liao, H. L. Wong, B.-P. Yang, and Y.-F. Yuan, "A transmitting boundary for transient wave analysis", *Sci. Sin., Ser. A*, vol. 27, no. 10, pp. 1063–1076, 1984.